

Chapter 1

Synthesis and Fabrication of Advanced Carbon Nanostructures



Anuj Kumar Tomar, Deepak Kumar, Akanksha Joshi, Gurmeet Singh, and Raj Kishore Sharma

1 Introduction

Different methods have been adopted by researchers for synthesis of carbon nanostructures; particularly, these synthesis methods are divided into two categories: One is bottom-up and second one is top-down approaches [1–6]. In the bottom-up approach, special emphasis will be given to the use of ionic liquids owing to their low volatility and hence allowing high-yield pyrolysis and covalent organic frameworks as a new low-temperature method for high structural control [7]. With a top-down approach, more focus will be on the metal organic frameworks as sacrificial templates and carbides for nanostructured carbon [8].

Bottom-up

- Chemical vapor deposition
- Sol–gel nanofabrication
- Laser pyrolysis synthesis
- Ionic liquid
- Covalent organic framework.

A. K. Tomar · D. Kumar · A. Joshi · G. Singh (✉) · R. K. Sharma (✉)
Department of Chemistry, University of Delhi, Delhi 110007, India
e-mail: gurmeet123@yahoo.com

R. K. Sharma
e-mail: drrajksharma@yahoo.co.in

A. K. Tomar
Department of Nano Convergence Engineering, Jeonbuk National University, Jeonju, Jeonbuk 54896, Republic of Korea

G. Singh
Pondicherry University, Chinna Kalapet, Kalapet, Puducherry 605014, India

Top-down

Lithography.

- Chemical/template etching
- MOF-derived carbon
- Carbide-derived carbon and carbon onion.

During the earth civilization, carbon has occupied a significant place mainly in the energy sector and has undergone a drastic transformation from coal as an energy source to activated carbon for electrical energy (batteries, solar cells, supercapacitor, etc.) [9]. The incredible properties of carbon to form linear (sp^1), planar (sp^2) and tetragonal configuration (sp^3), high abundance, and low specific weight have evoked great interest in the scientific community [10]. Over a few years, significant efforts have been made in the development of efficient carbon materials for different applications (energy storage, sensing, energy conversion, and harvesting, etc.); one of the advancements in this direction is the synthesis of carbon nanostructures. Low-dimensional materials with dimensions of structural elements (clusters, crystallites, or molecules) in the range of 1–100 nm are chiefly defined as nanostructured carbons. There is an entire range of dimensionality in the carbon nanostructures from zero-dimensional (fullerenes), one-dimensional (carbon nanotubes), two-dimensional (graphene sheets), to three-dimensional (fullerites, CNT ropes) with one another form “inverted carbons” that are basically mesoporous materials [11]. Nanodimension carbon structures comprise distinctiveness in the form of superior electrical conductivity, high surface area volume ratio, high porosity with outstanding mechanical, chemical, thermal, and optical properties [12]. In energy storage and conversion application, the role of nanostructuring is vast, and some of them are pointed here [13–16]:

- Nanostructuring provides more active sites for charge storage.
- High surface area owes to nanostructuring ensures a large contact between electrode and electrolyte.
- Stress generated during electrochemical reactions also gets reduced due to porous structure.
- Hollow and porous surfaces also provide spaces for filling other guest materials and hence can be used in multifunctional applications.
- Porous network also reduces the ionic diffusion length.

Hence, owing to these advantages, enormous research has been carried out to investigate the mechanism involved in controlling the dimension and surface chemistry of nanostructures. There are several ways in which nanostructuring can be done such as chemical vapor deposition, pyrolysis, covalent organic framework based, template oriented, and hydrothermal treatment, etc. [3]. On the basis of the process involved during synthesis, these methods are divided into two approaches: bottom-up and top-down. The bottom-up approach involves the building of structures from small atoms and molecules through covalent or other force interactions, whereas the top-down approach involves the etching of bulk structures to generate the needed

low-dimensional structures. Basically, the bottom approach is mainly focused on controlling the dimension, and a top-down approach is used to generate hollow or porous regions in the structures. However, with a top-down approach, the chances of defects generation and quantum effect increase due to the synthesis of small dimensions. The origination of defects with the nanostructuring would have an impact on the properties of carbon nanostructures. Therefore, in most cases, the combination of these approaches is carried out which is named a hybrid approach [17]. In this chapter, some of the particular bottom-up approaches and top-down approaches have been discussed that are majorly used by the researchers in pursuit of controlling the nanostructures.

Nanostructures are synthesized either by a bottom-up or top-down approach. The bottom-up approach relies on the attractive forces between the building blocks, whereas in the top-down approach, large materials are deconstructed to give nanostructures [5, 6]. Though these approaches comprise various synthesis methods, the chapter will be confined to some recent non-traditional synthesis methods.

2 Bottom-Up Approach

2.1 Chemical Vapor Deposition

In CVD, decomposition of gas-phase molecules to reactive species results in thin films with controlled stoichiometry and morphology. CVD allows for controlled deposition rates to give high-quality products having desired conformality [18]. Recently, the synthesis of carbon nanospheres via a non-catalytic chemical vapor deposition using low-rate acetylene gas with nitrogen gas was reported [19]. This strategy resulted in fluffy carbon nanospheres with spherical shape and regular size.

A new dimension to this synthesis method was added by Fischer and coworkers, where they combined CVD and template synthesis [20]. With this combined approach, graphitic carbon nanofibers were obtained. These are open-ended uniform hollow tubes and can be converted to carbon nanofibers with increasing deposition time. Although the crystallinity of CVD grown nanotubes is low, it is superior to other methods in terms of yield and purity.

2.2 Laser Pyrolysis

This is a recent method for the synthesis of nanoscale particles especially for carbides (Fig. 1). In laser pyrolysis, a dilute mixture of vaporized precursors is decomposed by a laser to initiate nucleation. These nuclei aggregate and transported by inert gas and depending on the amount of air different nanoparticles are formed. Owing to

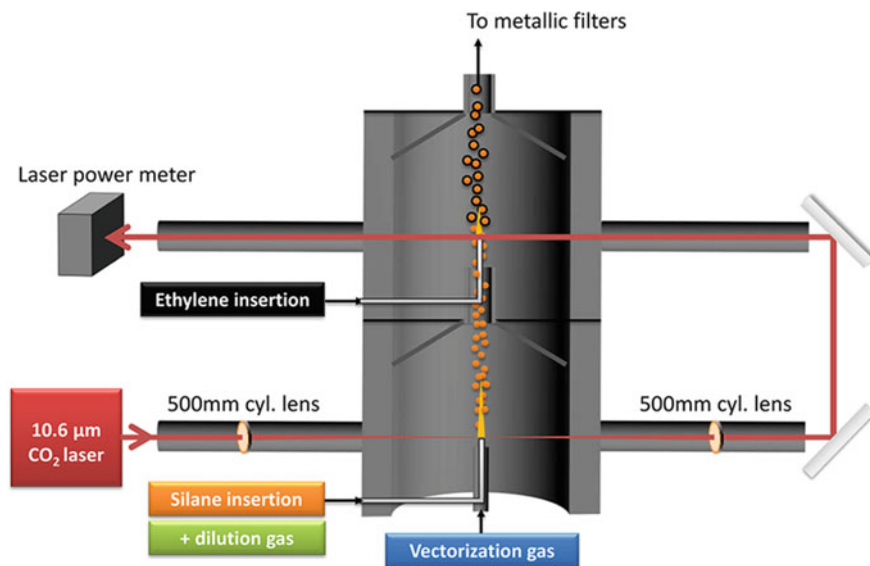


Fig. 1 Schematic representation of two-stage configuration reactor for laser pyrolysis. Reprinted with permission from Sourice et al. [21]. Copyright 2015 American Chemical Society

the fast nucleation and very short time in the reaction chamber, this method yields smaller nanoparticles than other vapor-phase methods.

One-step synthesis of silicon-carbon nanoparticles using laser pyrolysis was reported by Reynaud and coworkers [21]. The authors utilized a CO₂ laser to vaporize the reactants and beautifully utilized the working principle of laser pyrolysis. In the typical synthesis, firstly in the bottom stage, silicon cores are synthesized and transferred to the upper stage with a carrier gas where a carbon shell is deposited. This configuration prevents aerial oxidation of silicon surface. Silicon-carbon nanoparticles formed by this method were found to be very efficient for application in lithium-ion batteries with improved cycling stability.

2.3 Ionic Liquids

Although ionic liquids were discovered decades ago, their application to derive carbon materials is a relatively new emerging field. There are a variety of benefits that ILs offer,

- (i) most general is their negligible vapor pressure allowing much easier shaping, processing, and high yield under ambient thermal treatment,
- (ii) availability of a wide range of different cation/anion pairing enables a wide range of carbon nanostructures with varying heteroatoms,

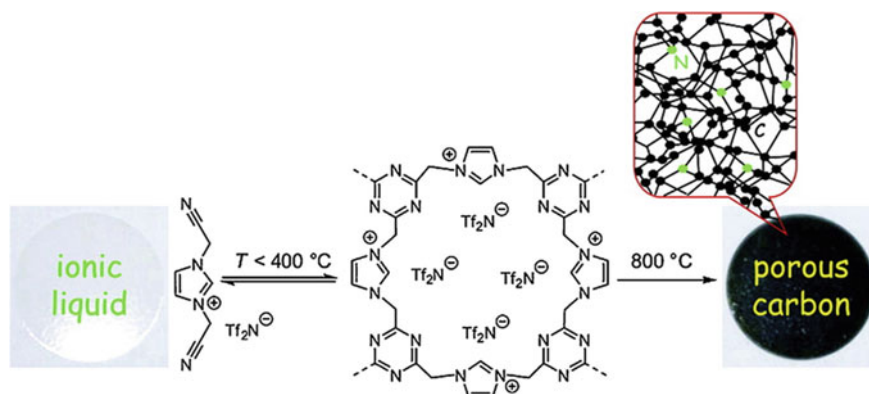


Fig. 2 Synthesis route for TSILs-derived N-doped porous carbon. Reprinted with permission from Lee et al. [23]. Copyright 2009 American Chemical Society

(iii) as ILs are good solvents so carbon composites with various other substances can be easily prepared by simply mixing.

Functional groups can be selectively introduced in ILs depending on the type of carbon required. Davis coined the term task-specific ionic liquids (TSILs) for ILs having specific functional groups attached for the desired property [22] as shown in Fig. 2. They selected ILs containing a nitrile group so that it can undergo cross-linking. They studied the effect of cations using 1-cyanomethyl-3-methylimidazolium [MCNIm]⁺ and 1,3-bis(cyanomethyl)imidazolium [BCNIm]⁺ and interestingly found that rather than cation, the surface properties of carbonaceous materials are affected to a great extent by anion. BET surface area of bis(trifluoromethylsulfoniylmide) ([Tf₂N]⁻) and Cl⁻ was found to be 700 m²/g and 10 m²/g, respectively [23]. Similarly, for [C(CN)₃]⁻ anion species, BET surface area was found to be 90 m²/g, whereas boron and nitrogen-doped carbon from [B(CN)₄]⁻ anion exhibits BET surface area of 500 m²/g [24].

Nowadays, ILs containing more than one type of cation/anion forming complex supramolecular structure, referred to as deep eutectic solvents (DES), were discovered. When quaternary ammonium salts in ILs complexes with hydrogen bond donors, then hydrogen bonding facilitates charge delocalization resulting in a eutectic mixture with a reduced melting point is formed.

Carbon and carbon-carbon nanotube composites can be obtained by using a choice of DES [25]. They utilized DES composed of ethylene glycol and CCl₄ to dissolve the reactants (resorcinol and formaldehyde). On heating monolith, resins were formed which were carbonized using thermal treatment. Results indicated high surface area for DES-based carbon monoliths than monoliths derived from aqueous media due to the structure effect of DES. Furthermore, it was found that MWCNTs form a homogeneous dispersion in DES by simple addition. This fact was observed in the SEM micrographs where MWCNTs were uniformly distributed in DES as compared to aqueous solvents.

Although ILs are gaining much importance for designing functional carbon materials, in-depth investigation of the correlation between precursor and carbon nanostructure is required to design novel need tailored materials.

2.4 Covalent Organic Frameworks (COFs)

Covalent organic frameworks are porous crystalline polymers composed of ordered periodic building block skeletons extended in 2/3-dimensions. They provide a low-temperature synthesis method for crystalline carbonaceous materials with a controlled structure. Based on the building blocks, different geometries and dimensions can be obtained. COFs are usually classified based on the linkage topology involved. These include (i) B–O (borates), (ii) C=N (imines), (iii) C=N_{aromatic} (azines), (iv) C=C (alkenes), (v) C–N (β -ketoenamines), and (vi) B=N (borazines) [26]. Among these, C–N linkage possess high structural stability even in strong acids.

Depending on the requirement, robust materials can be designed by Schiff's base reaction of amines with aldehydes resulting in imines. Based on this strategy, Feng group reported the synthesis of the wafer-sized multifunctional conjugated polymer [27]. They carried out this synthesis of the 2D multifunctional polymer at the air–water interface by Schiff's base polycondensation. Owing to the high stability of C=N, this polymer possesses a Young's modulus comparable to graphene and conjugation lowers the band gap to 1.4 eV making it suitable for semiconductors.

3 Top-Down Approach

3.1 Lithography

The term lithography originated from the Greek word *lithos* meaning stone and *graphein* meaning to write. Traditional lithography can generate various patterns by masking the required material and etching the exposed surface. Etching can be done by either chemicals or mechanically using high-energy electron beams. This gives rise to different types of lithography like optical lithography, soft lithography, block copolymer lithography, scanning probe, nanoimprint lithography, etc. Here, we will restrict our discussion to the recently emerged advanced technique, nanoimprint lithography (NIL) only. This is the most important lithographic technique for designing advanced nanostructures due to its ability to generate high-resolution nanopatterns with high throughput and low cost [28]. In conventional methods, the resolution is limited due to diffraction or beam scattering but in NIL, there is no such restriction. In NIL, a nanostructured mold is pressed on substrate precoated with a polymeric material. NIL is further classified as—thermoplastic, photo, and electrochemical NIL. In thermoplastic NIL, the substrate is modified with a thin layer of a

thermoplastic polymer. This is pressed with a patterned mold at the desired pressure. On heating, the polymer above glass transition temperature results in the required pattern on polymer [29]. In photo NIL, a substrate is modified with a photo-sensitive resist, and the mold is made transparent. After pressing in UV light, the resist becomes solid, and the pattern is transferred. Usually, polydimethylsiloxane (PDMS) is used for the transparent stamp as it offers a high-resolution pattern, and its low surface energy makes it easy to separate [30]. Fang group reported the use of stamps made of silver sulfide, a superionic conductor using electrochemical nanoimprint lithography (ECNIL) [31]. Henceforth pressing, when voltage is applied, it results in electrochemical etching to give the required pattern. Using ECNIL, three-dimensional micro-nanostructures (3D-MNS) were synthesized where ECNIL allowed for the synthesis of 3D-MNS with multilevel and continuously curved profiles on a crystalline GaAs wafer [32]. This suggests the high potential of ECNIL in semiconductor materials.

3.2 MOF-Derived Carbons

Metal organic frameworks (MOFs) consist of a regular array of metal ions and organic linkers to give crystalline porous materials [33, 34]. Uniform pore structure with tunable porosity makes them attractive candidates for various applications. To derive high surface area carbon, they can be directly carbonized or can be used as a template [35–38]. In 2008, the first synthesis of porous carbon from the MOF template was reported [35]. They carbonized furfuryl alcohol (additional carbon source) filled MOF-5 at 1000 °C. Such a high temperature helped in removing vaporized Zn metal with inert gas flow and attained metal-free carbon. The resulting carbon exhibited a high specific surface area of 2872 m² g⁻¹, useful for charge storing applications. This process was further refined by selecting particular MOFs to reduce the need of additional carbon sources to reduce the number of steps involved. It was found that using ZIF-8 as precursor, high surface area (3148 m² g⁻¹) carbon can be obtained without additional carbon [39].

Later on, it was realized that for some applications, bare carbon is not sufficient, and some heteroatoms may be useful for chemical functionalities and desired properties; heteroatom-doped carbon materials were searched. Here, zeolitic imidazole frameworks (ZIFs) seemed to be a suitable precursor for such materials. The same can be achieved by encapsulating the desired heteroatom rich molecule in MOF pores and then carbonizing the MOF. Using this strategy, synthesis of N, P, and S ternary-doped metal-free carbon from MOF was reported previously [40]. They selected MOF-5 as a template with dicyandiamide, with two heteroatom precursors (triarylphosphine and dimethylsulphoxide) to give high-performance carbon owing to the synergistic effect of heteroatoms (Fig. 3).

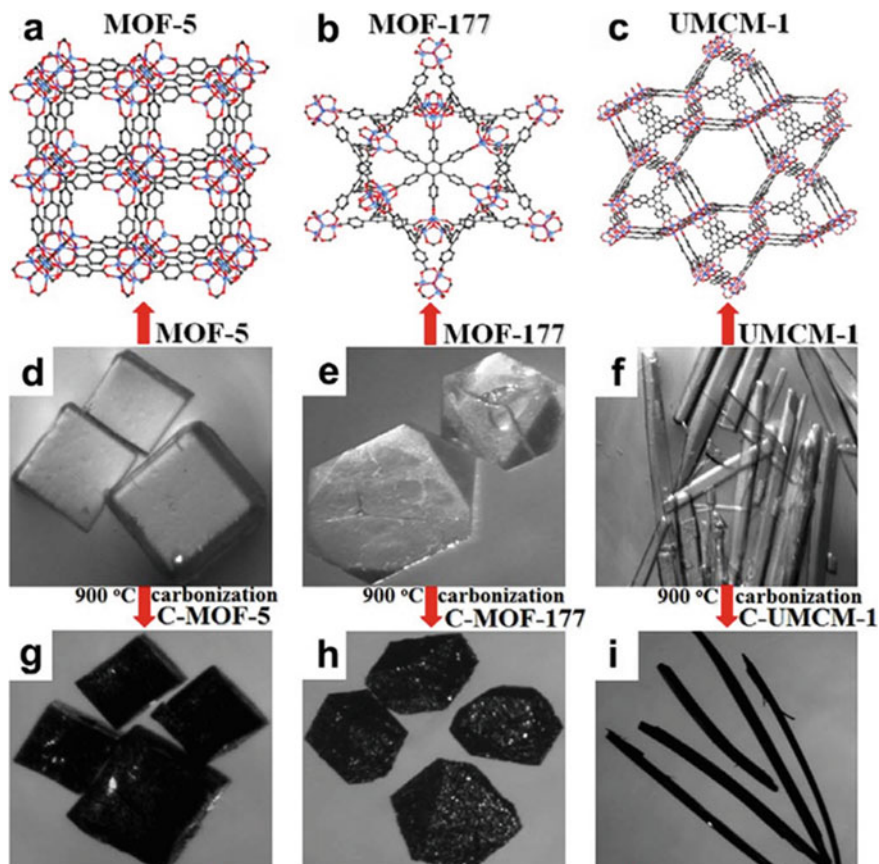


Fig. 3 a–c Representative 3D structures, d–i optical micrographs before and after carbonization for MOF-5, MOF-177, and UMCM-1. Reprinted with permission from Li et al. [40]. Copyright 2014 Springer Nature

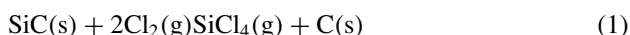
Although MOFs offer several advantages over traditional methods like tunable morphology, porosity, and heteroatom doping, there are some challenges to be considered. There is a strong need for low-cost synthesis methods for MOFs, and also, high-temperature carbonization makes it difficult to have full control over morphology. So, low temperature and cost-effective methods are required to expand the use of MOFs.

3.3 Carbide-Derived Carbon (CDC)

CDC is a collective term used for carbon derived from binary/ternary carbides (MAX phase) [41]. Depending on the method of metal removal and various experimental conditions, a variety of carbon nanostructures can be obtained. In this method, selective removal of metal atoms does not disturb the parent structure. The most common methods used in CDC are halogenation, hydrothermal treatment, and vacuum decomposition [42].

(i) Halogenation

Selective removal of metal atoms from carbide was first reported in 1918 [43]. In this method, carbon was formed as a byproduct of treating dry chlorine gas with hot silicon carbide.



Annealing of resulting porous carbon will remove residual chlorine. Halogenation of carbides up to 1000 °C produces disordered carbon, whereas above 1000 °C graphitization predominates. Although fluorine can also be used for some metal carbides but direct fluorination is aggressive and will result in either fluorocarbon or disintegrated SiC films. Using XeF₂ for etching was found to produce non-fluorinated SiC that also at low temperature (120 °C) than the conventional chlorination method [44]. These equations and the choice of halogen become more complex in the case of ternary carbides due to the possibility of the formation of more than one solid reaction product.

CDC formation from carbides through halogenation is also known as conformal transformation as it maintains the shape and volume of the parent carbide precursor [45, 46]. This fact was recently confirmed that even for a carbide precursor-like β-SiC having complex morphology, it maintains it on chlorination [47] (Fig. 4). A similar conformal transformation was observed for polymer-derived carbides (PDC) also [48, 49].

The structure of CDC mainly depends on carbide precursor and temperature. For TiC, the effect of halogenation temperature was studied and the results indicated that with increase in temperature, there is a constant increase in ordered structure (Fig. 5). Whereas at low temperatures, amorphous carbon was found. These results were further supported by quenched molecular dynamics (QMD) studies [50, 51].

(ii) Hydrothermal treatment

The hydrothermal method was first described for the synthesis of Tyranno (Si–Ti–C–O) fibers in the 1990s. In this method, the metal carbides area is treated with supercritical water at high pressure in the temperature range of 200–1000 °C [52, 53]. Jacobson performed Gibbs energy minimization for a large number of metal carbides at various temperatures and pressures under hydrothermal conditions [54] and found some common reaction products including carbon, MO_x, CH₄, CO₂, CO, and H₂ according to the following equations:

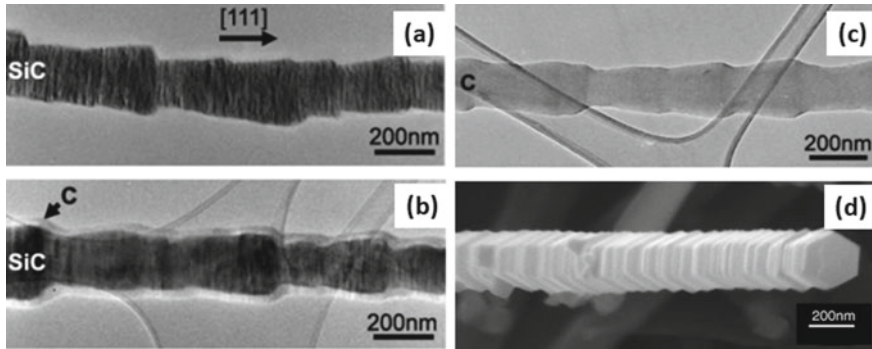


Fig. 4 TEM micrographs of β -SiC at various chlorination stages, **a** as received, **b** chlorinated at 700 °C, and **c** at 1200 °C. **d** SEM micrograph showing the conformal transformation. Reprinted with permission from Cambaz et al. [47]. Copyright 2006 John Wiley and Sons

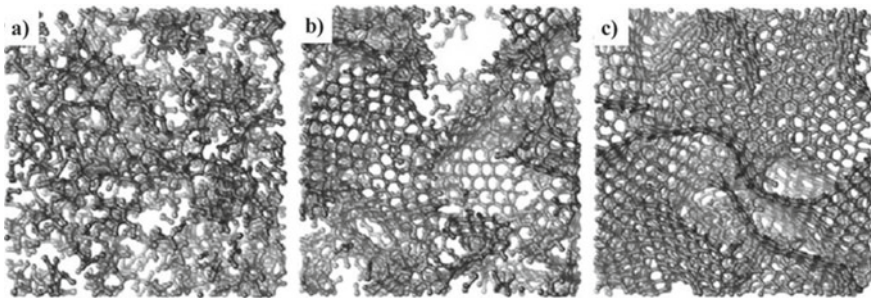
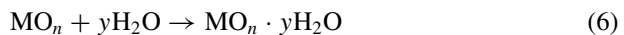
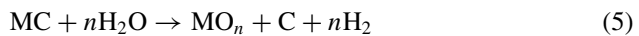
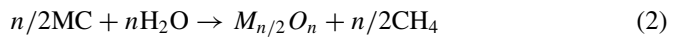


Fig. 5 Simulated structures of TiC-CDC quenched at different rates **a** 600 °C/fast quenching, **b** 800 °C/medium quenching, and **c** 1200 °C/slow quenching. Reprinted from Palmer et al. [51]. Copyright 2010 Elsevier



Experimental studies indicated that water/carbide (SiC) ratio is an important factor for deciding the yield. When this ratio is small, both carbon and silica are deposited

and for intermediate ratio both are formed but due to excess of water, silica gets dissolved. At a high ratio, neither carbon nor silica was formed.

The hydrothermal method produces amorphous carbon as indicated by the appearance of D and G bands in the Raman spectra of the product. But in the case of ternary carbides, the metal oxide phase may be present. As in Ti_3Si_2C , on hydrothermal treatment rutile/anatase was reported along with carbon [55]. The use of organic compounds like polyethylene was found to produce carbon nanotubes [56].

(iii) Thermal decomposition

Metal carbides on thermal decomposition in the vacuum will also generate CDC. It is based on the principle of incongruent decomposition. As the melting of carbon is higher than that of carbide, it remains while carbide evaporates. This method is also a conformal process like halogenation, and due to high temperatures, carbon nanostructures thus produced are more ordered. Using this method, Kusunoki group reported epitaxial carpets of self-organized carbon nanotubes (CNTs) from SiC [57]. Interestingly, this was the first time when no metal catalyst was used to obtain CNTs of the same chirality. They also presented a model to explain the mechanism of CNT formation based on residual oxygen. According to this, residual oxygen is the driving force; at low temperatures ($< 1000\text{ }^\circ\text{C}$), only graphite sheets are formed no CNT were formed. At temperatures around $1300\text{ }^\circ\text{C}$, there is SiO gas generated which forms nanotubes (Fig. 6).

This method can also be used to produce graphene from SiC either by vacuum decomposition or heating in an inert environment. Its formation mechanism is as that for CNT assuming that prior to CNT formation, there is the formation of a thin graphene layer [58–61].

Comparisons of various properties are given in Table 1.

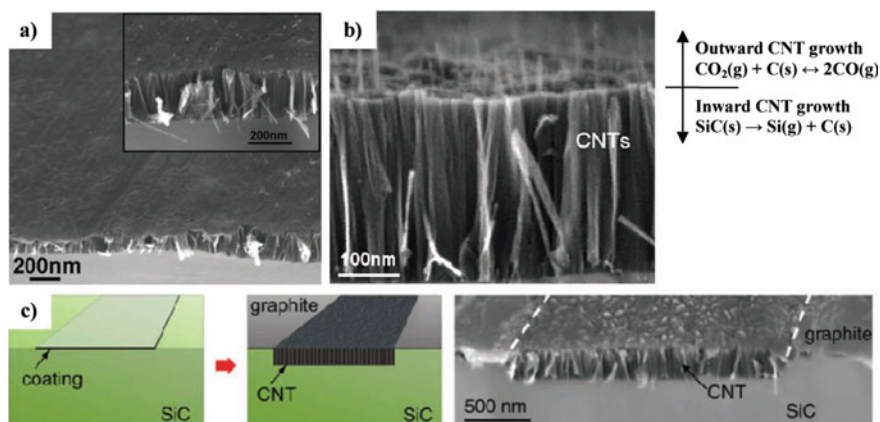


Fig. 6 SEM micrographs of vacuum decomposed 6H-SiC carbon nanostructures for **a** C-face oriented in high vacuum and **b** Si-face oriented in low vacuum. **c** Effect of surface modification on CNT growth. Reprinted with permission from Cambaz et al. [50]. Copyright 2008 Elsevier

Table 1 Comparison of various properties of carbon materials discussed

Sr. No.	Precursor	Active material	Surface are ($\text{m}^2 \text{g}^{-1}$)/diameter (nm)	Application	References
1	Acetylene and nitrogen	Carbon nanospheres	100–200 nm	Sensors, photo-catalysis, and opto-electronic devices	[19]
2	C_2H_4 and SiH_4	Carbon covered silicon nanoparticles	$156 \text{ m}^2 \text{ g}^{-1}$	Li-ion batteries	[21]
3	Task specific ionic liquid	N-doped carbon	$\leq 800 \text{ nm}$	Carbon coating, CO_2 capture	[23]
4	Ionic liquids	Boron and nitrogen rich carbon	$537 \text{ m}^2 \text{ g}^{-1}$	CO_2 adsorption, CO_2/N_2 separation	[24]
5	Resorcinol–formaldehyde	Carbon–carbon nanotube	$350 \text{ m}^2 \text{ g}^{-1}$	–	[25]
6	Covalent organic framework	2D-conjugated polymer	–	Semiconductor, electrocatalysis	[27]
7	Metal organic framework	Porous carbon	$2872 \text{ m}^2 \text{ g}^{-1}$	Supercapacitor	[35]
8	Metal organic framework	Nonporous carbon	$3405 \text{ m}^2 \text{ g}^{-1}$	Supercapacitor, hydrogen storage	[39]
9	Metal organic framework	Heteroatom-doped porous carbon	$548 \text{ m}^2 \text{ g}^{-1}$	Electrocatalysis	[40]
10	Carbide-derived carbon	Carbon fibers	$3116 \text{ m}^2 \text{ g}^{-1}$	Adsorption	[48]

Using the above methods, a variety of carbon nanostructures can be synthesized. Aggregation of atomic sheets of 2D materials like graphene hinders its applications and requires advanced methods to prevent it. Some important methods are:

(1) Shape/orientation modified growth of graphene

Synthesis of graphene directly on the substrate leads to restacking but one way to avoid this is to synthesize vertically oriented graphene. Using the CVD method, vertically oriented graphene was synthesized on Ni substrate where mostly edges are exposed and fully accessible [62]. On some substrates when this is not possible then instead of flat graphene sheets, modification of the shape of graphene to curved or crumpled sheets will also prevent aggregation. This modification provides additional surface area and pore volume essential for several applications [63].

(2) Intercalated graphene

After exfoliation, insertion of typical guest molecules in graphene interlayers is an effective strategy to prevent aggregation with a maintained flat sheets structure. To date, various spacers have been reported including metal nanoparticles, carbon nanotubes, conducting polymers, etc. Based on the type of application, the interlayer gallery height can be fine-tuned by selecting definite spacers. Recently, polyoxometalates (an emerging class of materials) have been reported as a spacer [64]. Polyoxometalates not only prevented aggregation but also provided additional redox-active sites for charge storage.

(3) 3D interconnected graphene

This strategy is utilized in certain cases when no foreign element other than graphene is required. Interconnection of a large number of 2D nanosheets results in a complex 3D network. In this complex network, each graphene sheet is supported by other sheets, resulting in a porous structure having a very low tendency to aggregate. Although there are a variety of materials reported with the 3D networks, graphene hydrogels are the important ones. In the simplest way, hydrothermal reduction of graphene oxide will induce cross-linking at multiple points leading to the hydrogel. This generates a porous structure with vast pore size distribution making it useful for a large number of applications [65].

4 Conclusion

The peculiar properties of carbon nanostructures require the attention of researchers to develop advanced synthesis approaches. There are many ways to synthesize carbon materials, where the structures and functions are governed by the processing conditions and precursors used. Depending on the requirement and initial conditions available, this chapter summarizes various methods for the top-down and bottom-up synthesis of carbon nanostructures. Among different approaches, some are outdated

and traditional methods that are inefficient to fulfill the present need of advanced nanostructures. This chapter discusses some of the recent methods comprising high yield and ecofriendly nature including laser pyrolysis, ionic liquids precursor, etc. Independently, both these approaches can generate different nanostructures with unique properties; however, they suffer from their limitations which demand consideration toward the generation of some new techniques comprising both top-down and bottom-up approaches for developing novel materials in various research fields.

Acknowledgements Authors gratefully acknowledge the financial support received from Science and Engineering Research Board Grant No. EMR/2016/002846. Financial support received from the Institute of Eminence is gratefully acknowledged. Deepak Kumar is grateful to CSIR for the financial support through SRF fellowship (09/045(1632)/2019-EMR-1). Akanksha Joshi thankfully acknowledges the financial support through SRF fellowship (09/045(1422)/2016-EMR-1).

References

1. Casco ME, Martínez-Escandell M, Gadea-Ramos E, Kaneko K, Silvestre-Albero J, Rodríguez-Reinoso F (2015) High-pressure methane storage in porous materials: are carbon materials in the pole position? *Chem Mater* 27:959–964
2. Sahu V, Shekhar S, Sharma RK, Singh G (2015) Ultrahigh performance supercapacitor from lacey reduced graphene oxide nanoribbons. *ACS Appl Mater Interfaces* 7(5):3110–3116
3. Borchardt L, Zhu QL, Casco ME, Berger R, Zhuang X, Kaskel S, Feng X, Xu Q (2017) Toward a molecular design of porous carbon materials. *Mater Today* 20:592–610
4. Joshi A, Sahu V, Singh G, Sharma RK (2019) Performance enhancement of a supercapacitor negative electrode based on loofah sponge derived oxygen rich carbon through encapsulation of MoO₃ nanoflowers. *Sustainable Energy Fuels* 3:1248–1257
5. Bellah MM, Chistensen SM, Iqbal SM (2012) Nanostructures for medical diagnostics. *J Nanomater*
6. Yu HD, Regulacio MD, Ye E, Han MY (2013) Chemical routes to top-down nanofabrication. *Chem Soc Rev* 42(14):6006–6018
7. Wan MM, Sun XD, Li YY, Zhou J, Wang Y, Zhu JH (2016) Facilely fabricating multifunctional N-enriched carbon. *ACS Appl Mater Interfaces* 8:1252–1263
8. Sato H, Matsuda R, Sugimoto K, Takata M, Kitagawa S (2010) Photoactivation of a nanoporous crystal for on-demand guest trapping and conversion. *Nat Mater* 9:661–666
9. Yang Z, Ren J, Zhang Z, Chen X, Guan G, Qiu L, Zhang Y, Peng H (2015) Recent advancement of nanostructured carbon for energy applications. *Chem Rev* 115(11):5159–5223
10. Sun Q, Zhang R, Qiu J, Liu R, Xu W (2018) On-surface synthesis of carbon nanostructures. *Adv Mater* 30:1705630
11. Hoseisel TN, Schreftl S, Szilluweit R, Frauenrath H (2010) Nanostructured carbonaceous materials from molecular precursors. *Angew Chem Int Ed* 49:6496–6515
12. Kwiatkowski M, Policicchio A, Seredych M, Bandosz TJ (2016) Evaluation of CO₂ interactions with S-doped nanoporous carbon and its composites with a reduced GO: effect of surface features on an apparent physical adsorption mechanism. *Carbon* 98:250–258
13. Joshi A, Singh G, Sharma RK (2020) Engineering multiple defects for active sites exposure towards enhancement of Ni₃S₂ charge storage characteristics. *Chem Eng J* 384:123364
14. Joshi A, Lalwani S, Singh G, Sharma RK (2019) Highly oxygen deficient, bimodal mesoporous silica-based supercapacitor with enhanced charge storage characteristics. *ElectrochimActa* 297:705–714

15. Tomar AK, Joshi A, Singh G, Sharma RK (2020) Triple perovskite oxide as an advanced pseudocapacitive material: multifarious element approach with an ordered structure. *J Mater Chem A* 8:24013–24023
16. Joshi A, Tomar AK, Singh G, Sharma RK (2021) Engineering oxygen defects in the boron nanosheet for stabilizing complex bonding structure: an approach for high-performance supercapacitor. *Chem Eng J* 407:127122
17. Wei Q, Xiong F, Tan S, Huang L, Lan EH, Dunn B, Mai L (2017) Porous one-dimensional nanomaterials: design, fabrication and applications in electrochemical energy storage. *Adv Mater* 29:1602300
18. Sun L, Yuan G, Gao L, Yang J, Chhowalla M, Gharahcheshmeh MH, Liu Z (2021) Chemical vapour deposition. *Nat Rev Methods Primers* 1(5)
19. Faisal AD, Aljubouri AA (2016) Synthesis and production of carbon nanospheres using noncatalytic CVD method. *Int J Adv Mater Res* 2(5):86–91
20. Che G, Lakshmi BB, Martin CR, Ruoff RS, Fisher ER (1998) Chemical vapor deposition-based synthesis of carbon nanotubes and nanofibers using a template method. *Chem Mater* 10:260–267
21. Sourice J, Quinsac A, Leconte Y, Sublemontier O, Porcher W, Haon C, Bordes A, Vito ED, Boulineau A, Larbi SJS, Herlin-Boime N, Reynaud C (2015) One-step synthesis of Si@C nanoparticles by laser pyrolysis: high-capacity anode material for lithium-ion batteries. *ACS Appl Mater Inter* 7:6637–6644
22. Davis JHJ (2004) Task-specific ionic liquids. *Chem Lett* 33(9):1072–1077
23. Lee JS, Wang X, Luo H, Baker GA, Dai S (2009) Facile ionothermal synthesis of microporous and mesoporous carbons from task specific ionic liquids. *J Am Chem Soc* 131(13):4596–4597
24. Fulvio PF, Lee JS, Mayes RT, Wang X, Mahurin SM, Dai S (2011) Boron and nitrogen-rich carbons from ionic liquid precursors with tailorable surface properties. *PhysChemChemPhys* 13:13486–13491
25. Gutierrez MC, Rubio F, del Monte F (2010) Resorcinol-formaldehyde polycondensation in deep eutectic solvents for the preparation of carbons and carbon-carbon nanotube composites. *Chem Mater* 22:2711–2719
26. Diercks CS, Yaghi OM (2017) The atom, the molecule, and the covalent organic framework. *Science* 355:eaal1585
27. Sahabudeen H, Qi H, Glatz BA, Tranca D, Dong R, Hou Y, Zhang T, Kuttner C, Lehnert T, Seifert G, Kaiser U, Fery A, Zheng Z, Feng X (2016) Wafer-sized multifunctional polyimine-based two-dimensional conjugated polymers with high mechanical stiffness. *Nat Commun* 7:13461
28. Chou SY, Krauss PR, Renstrom PJ (1996) Imprint lithography with 25-nanometer resolution. *Science* 272:85–87
29. Barcelo S, Li Z (2016) Nanoimprint lithography for nanodevice fabrication. *Nano Converg Korea Nano Technol Res Soc* 3(1):21
30. Traub MC, Longsine W, Truskett VN (2016) Advances in nanoimprint lithography. *Annu Rev Chem Biomol Eng* 7(1):583–604
31. Hsu KH, Schultz PL, Ferreira PM, Fang NX (2007) Electrochemical nanoimprinting with solid-state superionic stamps. *Nano Lett* 7(2):446–451
32. Zhang J, Zhang L, Han L, Tian ZW, Tian ZQ, Zhan D (2017) Electrochemical nanoimprint lithography: when nanoimprint lithography meets metal assisted chemical etching. *Nanoscale* 9:7476–7482
33. Furukawa H, Cordova KE, O’Keeffe M, Yaghi OM (2013) The chemistry and applications of metal-organic frameworks. *Science* 341:1230444
34. Zhu QL, Xu Q (2014) Metal-organic framework composites. *Chem Soc Rev* 43(16):5468–5512
35. Liu B, Shioyama H, Akita T, Xu Q (2008) Metal-organic framework as a template for porous carbon synthesis. *J Am Chem Soc* 130(16):5390–5391
36. Xia W, Mahmood A, Zou R, Xu Q (2015) Metal-organic frameworks and their derived nanostructures for electrochemical energy storage and conversion. *Energy Environ Sci* 8:1837–1866

37. Shen K, Chen X, Chen J, Li Y (2016) Development of MOF-derived carbon-based nanomaterials for efficient catalysis. *ACS Catal* 6(9):5887–5903
38. Wang H, Zhu QL, Zou R, Xu Q (2017) Metal-organic frameworks for energy applications. *Chem* 2(1):52–80
39. Jiang HL, Liu B, Lan YQ, Kuratani K, Akita T, Shioyama H, Zong F, Xu Q (2011) From metal-organic framework to nanoporous carbon: toward a very high surface area and hydrogen uptake. *J Am Chem Soc* 133(31):11854–11857
40. Li JS, Li SL, Tang YJ, Li K, Zhou L, Kong N, Lan YQ, Bao JC, Dai ZH (2014) Heteroatoms ternary-doped porous carbons derived from MOFs as metal-free electrocatalysts for oxygen reduction reaction. *Sci Rep* 4:5130
41. Presser V, Heon M, Gogotsi Y (2011) Carbide-derived carbons—from porous networks to nanotubes and graphene. *Adv Funct Mater* 21(5):810–833
42. Roy R, Ravichandran D, Badzian A, Breval E (1996) Attempted hydrothermal synthesis of diamond by hydrolysis of b-SiC powder. *Diam Relat Mater* 5(9):973–976
43. Hutchins O (1918) US Patent 1271713
44. Batisse N, Guerin K, Dubois M, Hamwi A, Spinelle L, Tomasella E (2010) Fluorination of silicon carbide thin films using pure F₂ gas or XeF₂. *Thin Solid Films* 518:6746
45. Chen L, Behlau G, Gogotsi Y, McNallan MJ (2003) Carbothermal synthesis of boron nitride coatings on silicon carbide. *J Am Ceram Soc* 86(11):1830–1837
46. Ersoy DA, McNallan MJ, Gogotsi YG (2001) Carbon coatings produced by high temperature chlorination of silicon carbide ceramics. *Mater Res Innov* 5:55–62
47. Cambaz ZG, Yushin GN, Gogotsi Y, Vyshnyakova KL, Pereselentseva LN (2006) Formation of carbide-derived carbon on β -silicon carbide whiskers. *J Am Ceram Soc* 89:509
48. Rose M, Kockrick E, Senkovska I, Kaskel S (2010) High surface area carbide-derived carbon fibers produced by electrospinning of polycarbosilane precursors. *Carbon* 48(2):403–407
49. Yeon SH, Reddington P, Gogotsi Y, Fischer JE, Vakifahmetoglu C, Colombo P (2010) Carbide-derived-carbons with hierarchical porosity from a preceramic polymer. *Carbon* 48:201–210
50. Cambaz ZG, Yushin G, Osswald S, Mochalin V, Gogotsi Y (2008) Noncatalytic synthesis of carbon nanotubes, graphene and graphite on SiC. *Carbon* 46:841–849
51. Palmer JC, Llobet A, Yeon SH, Fischer JE, Shi Y, Gogotsi Y, Gubbins KE (2010) Modeling the structural evolution of carbide-derived carbons using quenched molecular dynamics. *Carbon* 48:1116–1123
52. Gogotsi Y, Yoshimura M (1994) Formation of carbon films on carbides under hydrothermal conditions. *Nature* 367:628–630
53. Gogotsi Y, Yoshimura M (1994) Water effects on corrosion behavior of structural ceramics. *MRS Bull* 19(10):39–45
54. Jacobson NS, Gogotsi YG, Yoshimura M (1995) Thermodynamic and experimental study of carbon formation on carbides under hydrothermal conditions. *J Mater Chem* 5:595–601
55. Zhang H, Presser V, Berthold C, Nickel KG, Wang X, Raisch C, Chasse T, He L, Zhou Y (2010) Mechanisms and kinetics of the hydrothermal oxidation of bulk titanium silicon carbide. *J Am Ceramic Soc* 93(4):1148–1155
56. Gogotsi Y, Libera JA, Naguib N (2002) In situ chemical experiments in carbon nanotubes. *Chem Phys Lett* 365(3–4):354–360
57. Kusunoki M, Rokkaku M, Suzuki T (1997) Epitaxial carbon nanotube film self-organized by sublimation decomposition of silicon carbide. *Appl Phys Lett* 71:2620
58. Emtsev K, Bostwick A, Horn K, Jobst J, Kellogg G, Ley L, McChesney J, Ohta T, Reshanov S, Röhrl J, Rotengerg E, Schmid AK, Waldmann D, Weber HB, Seyller T (2009) Towards wafer-size graphene layers by atmospheric pressure graphitization of silicon carbide. *Nat Mater* 8:203–207
59. Van Bommel AJ, Crombeen JE, Van Tooren A (1975) LEED and Auger electron observations of the SiC(0001) surface. *Surf Sci* 48(2):463–472
60. Rollings E, Gweon GH, Zhou SY, Mun BS, Mc-Chesney JL, Hussain BS, Fedorov AV, First PN, de Heer WA, Lanzara A (2006) Synthesis and characterization of atomically thin graphite films on a silicon carbide substrate. *J Phys Chem Solids* 67(9–10):2172–2177

61. Virojanadara C, Syväjärvi M, Yakimova R, Johansson LI, Zakharov AA, Balasubramanian T (2008) Homogeneous large-area graphene layer growth on 6H-SiC(0001). *Phys Rev B* 78:245403
62. Miller JR, Outlaw RA, Holloway BC (2010) Graphene double-layer capacitor with ac line-filtering performance. *Science* 329:1637–1639
63. Liu C, Yu Z, Neff D, Zhamu A, Jang BZ (2010) Graphene-based supercapacitor with an ultrahigh energy density. *Nano Lett* 10:4863–4868
64. Kumar D, Tomar AK, Singal S, Singh S, Sharma RK (2020) Ammonium decavanadate nanodots/reduced graphene oxide nanoribbon as “inorganic-organic” hybrid electrode for high potential aqueous symmetric supercapacitors. *J Power Sources* 462:228173
65. Xu Y, Sheng K, Li C, Shi G (2010) Self-assembled graphene hydrogel via a one-step hydrothermal Process. *ACS Nano* 4:4324–4330